

Magnetic field dependence of the dynamics of ^{87}Rb spin-2 Bose-Einstein condensates

T. Kuwamoto,* K. Araki, T. Eno, and T. Hirano

Department of Physics, Gakushuin University, 1-5-1 Mejiro, Toshima-ku, Tokyo 171-8588, Japan

(Received 30 January 2004; published 8 June 2004)

We experimentally studied the spin-dependent collision dynamics of ^{87}Rb spin-2 Bose-Einstein condensates confined in an optical trap. The condensed atoms were initially populated in the $|F=2, m_F=0\rangle$ state, and their time evolutions in the trap were measured in the presence of external magnetic field strengths ranging from 0.1 to 3.0 G. The atom loss rate due to inelastic two-body collisions was found to be $1.4(2) \times 10^{-13} \text{ cm}^3 \text{ s}^{-1}$. Spin mixing in the $F=2$ manifold developed dramatically for the first few tens of milliseconds, and the oscillations in the population distribution between different magnetic components were observed over a limited range of magnetic field strengths. The antiferromagnetic property of this system was deduced from the magnetic field dependence on the evolution of relative populations for each m_F component.

DOI: 10.1103/PhysRevA.69.063604

PACS number(s): 03.75.Mn, 34.50.Pi, 05.30.Jp

I. INTRODUCTION

Multicomponent Bose-Einstein condensates produced from dilute atomic gases have opened up new fields for the study of quantum matter waves and superfluids. The first reports of the use of these systems were made by the JILA group [1] using ^{87}Rb condensates confined in a magnetic trap. Sympathetic cooling and, later, two-photon transitions [2] were applied to produce two-component condensates comprised of two hyperfine spin states. The system produced in that study is regarded as a spin-1/2 condensate, and a large number of interesting studies such as vortex formation [3] and spatial resolution of spin waves [4] have been carried out since then. However, in this system, the atoms are fixed in weak-seeking magnetic states, and external fields such as microwaves are required to couple each of the components.

In contrast, an optical trap enables confinement of the atoms in all the magnetic substates; i.e., the internal spin degrees of freedom caused by the hyperfine spin of the atoms are liberated. Under these conditions, the condensed atoms in a magnetic substate can be converted into atoms in other substates through interatomic interactions in the absence of external coupling fields. The ground- and excited-state structures can be determined according to their magnetic and topological properties [5–8]. The MIT group was the first to succeed in optically confining Na spin-1 condensates [9]. Since then, that group has studied the ground-state structure [10], metastability [11], and quantum tunneling [12] of Na spinor condensates. Recent investigations of ^{87}Rb spin-1 condensates have shown that their magnetization is ferromagnetic [13,14].

The spin-2 condensate is a more attractive system, because it is thought to have a new magnetic response. Koashi and Ueda [8] and Ciobanu *et al.* [15] reported that spin-singlet “trios” (cyclic states) can be formed in this system. Furthermore, a rich variety of spinor dynamics is expected from spin-2 condensates with greater spin values than those reported for other systems. To date, a number of theoretical

[8,15–18] and experimental [13,14,19] investigations have been conducted on this system. In particular, the Hamburg group has recently measured the spinor dynamics of ^{87}Rb spin-2 condensates at a fixed magnetic field strength and reported evidence of antiferromagnetic behavior [13].

In this paper, we experimentally investigate the spin-mixing dynamics and trap loss of optically confined ^{87}Rb spin-2 condensates at various magnetic field strengths. Initially, condensates in which almost all of the atoms were polarized in the $|F=2, m_F=0\rangle$ state were prepared in a trap. We confirmed that the trap loss rate in this state is two orders of magnitude higher than in the stretched states ($m_F = +2$ and -2 states), due to inelastic two-body collisions. The magnetic field and atomic density dependence on the spinor dynamics in the $F=2$ manifold were also demonstrated. Furthermore, we discuss the ground-state magnetic properties of the system by investigating changes in the spin-mixing rates at various magnetic field strengths.

II. THEORETICAL BACKGROUND

A condensate with spin degrees of freedom is represented by a vector order parameter that is symmetrical under rotation in the hyperfine spin space of a zero-strength magnetic field and has $2F+1$ components, where F is the hyperfine spin. The mean-field theory was extended with the vector order parameter, and various properties of spinor condensates have been theoretically suggested [6–8,15–18]. The ground-state structure of a spinor condensate is formed as minimizing the spin-dependent interatomic interaction energy. For the $F=2$ system, taking into account the effects of an external magnetic field, the energy is characterized by the following function [8,13,18]:

$$\epsilon_{spin} = c_1 \langle \vec{F} \rangle^2 + \frac{4}{5} c_2 \langle s_- \rangle - p \langle F_z \rangle - q \langle F_z^2 \rangle, \quad (1)$$

where $\langle \vec{F} \rangle$, $\langle F_z \rangle$, and $\langle s_- \rangle$ denote the average spin, z component, and spin-singlet pair amplitude, and p and q correspond to the linear and quadratic Zeeman energies, respectively. c_1 and c_2 are parameters that characterize the spin-dependent

*Electronic address: kuwamoto@qo.phys.gakushuin.ac.jp

mean-field energies and are defined by the s -wave scattering lengths a_f for binary collisions with total spin f as follows [8,15]:

$$c_1 = \frac{4\pi\hbar^2 a_4 - a_2}{m \cdot 7}, \quad c_2 = \frac{4\pi\hbar^2 7a_0 - 10a_2 + 3a_4}{m \cdot 7}, \quad (2)$$

where m denotes the mass of a rubidium atom.

The s -wave scattering lengths a_0 , a_2 , and a_4 were calculated by Klausen *et al.* [17] based on experimental results by Roberts *et al.* [20]. Using these results, the c_1 and c_2 values were calculated to be 9.2×10^{-20} Hz m³ and -1.5×10^{-19} Hz m³. Although these magnitudes are about 80 and 50 times smaller than the spin-independent mean-field coefficient [$c_0 = (4\pi\hbar^2/m)(4a_2 + 3a_4)/7$], their signs and relative magnitudes determine the dynamic and stationary properties as well as the magnetic responses of spin-2 condensates when the external magnetic field is either small or zero. The energy ranges of the first and second terms in Eq. (1) were estimated to be $k_B \times 0-4$ nK and $k_B \times 0-1$ nK using the initial mean atom density $n = 2.1 \times 10^{14}$ cm⁻³ in our experiments and the s -wave scattering lengths given in Ref. [17]. While the magnetization of ⁸⁷Rb spin-2 condensates has been predicted to be antiferromagnetic, their corresponding point in the phase diagram shown in Ref. [17] is very close to the cyclic phase. Thus, in order to determine conclusive criteria regarding the magnetization of this system, it is important to study the spinor dynamics at various magnetic field strengths.

The ground state of the system is formed by the total spin-conserved interactions between atoms such as $|2, 0\rangle + |2, 0\rangle \leftrightarrow |2, +1\rangle + |2, -1\rangle$, $|2, +1\rangle + |2, -1\rangle \leftrightarrow |2, +2\rangle + |2, -2\rangle$, and $|2, 0\rangle + |2, 0\rangle \leftrightarrow |2, +2\rangle + |2, -2\rangle$, assuming that we ignore the loss of atoms. We also note that there are several selection rules relating to the spin-exchange processes. The first term in Eq. (1) allows for the processes with $\Delta m_F = \pm 1$, and the second term allows for $\Delta m_F = \pm 2$ interactions [13].

III. EXPERIMENT

We used a simple double magneto-optical trap (MOT) apparatus to accumulate ultracold ⁸⁷Rb atoms. The atoms collected in the first MOT were continuously transferred to the second MOT by irradiating with a weak near-resonant cw laser beam focused on the center of the atomic cloud. More than 10^9 atoms can be collected in the second MOT over a time interval of 3 s. The atoms were then pumped optically into the $|2, +2\rangle$ state and recaptured in the Ioffe-Pritchard (clover-leaf) type magnetic trap. Bose-Einstein condensates containing 10^6 atoms were created by evaporative cooling with an rf field for 14 s.

The condensates were then loaded into an optical trap formed by two far off-resonant laser beams with a wavelength of 850 nm. One of the laser beams was irradiated along the long axis of the cigar-shaped condensates with a power of 7 mW and a $1/e^2$ radius at a focus of 24 μ m. The second laser with 11 mW of power was focused perpendicularly across the first beam, with a waist radius of 90 μ m. Under these conditions and taking into account the effect of

gravity, the potential depth of the trap is calculated to be about 1 μ K. The power fluctuations of both lasers were less than 1%. After the creation of the condensates, the power from both lasers was simultaneously ramped exponentially for 50 ms. The magnetic trap was then quickly turned off. A transfer rate of nearly 100% was achieved. The aspect ratio of the condensates in the trap was estimated to be 11, and the average trap frequency measured from the release energy of the condensates [9] was found to be 82 Hz.

We experimentally confirmed that all of the condensed atoms transferred to the optical trap populated in the $|2, -2\rangle$ state even though the condensed atoms were in the $|2, +2\rangle$ state in the magnetic trap. This occurred because when the magnetic trap was turned off, there was a slight delay in the switch-off timing of the current through the compensation coil pair, which was driven independently from the main coils of the magnetic trap and used to control the minimum field strength at the trap center. That is, because the direction of the magnetic field from the compensation coils was opposite to that of the field produced by the main coils (and also opposite to the magnetic field from the whole coils of magnetic trap) along the long axis of the cigar-shaped condensates, the field direction was nonadiabatically reversed when the magnetic trap was turned off, whereas the initial direction of the atomic spin did not change. We found that the condition of the atomic population did not affect our experiments, and we therefore used the condition described above.

Lifetime measurements were performed on the optically trapped condensates in the $|2, -2\rangle$ state. The $1/e$ lifetime of 4.0(1.6) s was obtained by applying an exponential fit to the data after excluding the initial faster decay part caused by inelastic three-body collisions. This value is shorter than that of the magnetic trap for which the lifetime was measured to be approximately 7 s. To explain this observation, we believe that the heating rate of the condensates increased in comparison to the magnetic trap, because noncondensed atoms were confined in the *arm region*, which is the noncrossed region of the two laser beams in a crossed-type optical trap [21]. The photon scattering rate was found to be 2×10^{-3} s⁻¹, and therefore the light absorption by atoms was ignored. The lifetime used in this study was sufficient, however, to measure the spinor dynamics under investigation.

To study the spinor dynamics, the condensates in the $|2, -2\rangle$ state were transferred to the $|2, 0\rangle$ state by sweeping the rf field through resonance in an external magnetic field of 20 G [22]. This field value allowed us to selectively prepare the desired states by quadratic Zeeman shifts. By controlling the sweep time, sweep range, and amplitude of the rf field, we achieved a transfer rate of more than 90%. The above manipulations were performed after 400 ms of transferring the condensates to the optical trap. After state preparation, the 20-G field was turned off, and accurately controlled external magnetic fields in the range from 0.1 to 3.0 G were immediately applied. Under these conditions, optically trapped condensates in the $|2, 0\rangle$ state evolved for a variable amount of time. The optical trap was turned off at the end of the time evolution period, and absorption imaging was applied after free expansion ranging from 15 to 22 ms to measure the population distribution of each spin component. The different spin components were then spatially separated using the Stern-Gerlach method [9].

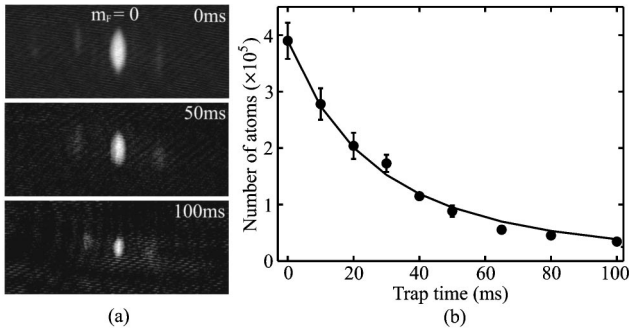


FIG. 1. Reduction in the number of condensed atoms in an optical trap at a magnetic field strength of 3.0 G. (a) Absorption images of atomic clouds after free expansions of 22 ms (upper two) and 18 ms (lowest one). Storage times are also shown on the right-hand side. A Stern-Gerlach separation was applied to distinguish the different m_F components. $|2,0\rangle$ was the predominant component observed. The size of the field of view for each image is 1.1×0.45 mm. (b) Number of condensed atoms in the $|2,0\rangle$ state remaining in the trap as a function of trap time. Each data point represents the average of three measurements. Error bars indicate the standard deviation. The curve was fitted to Eq. (3), after omitting the K_1 and K_3 terms.

The residual magnetic field of 10 mG was measured with microwave transitions between the $F=2$ and $F=1$ hyperfine states of the optically confined condensates. We also estimated the residual gradient field, using a Hall probe magnetometer, to be 30 mG/cm.

IV. RESULTS AND DISCUSSION

We first demonstrate the time evolution of optically confined condensates initially prepared in the $|2,0\rangle$ state in a magnetic field strength of 3.0 G. Figure 1(a) depicts the time-of-flight absorption images taken after various evolution times. Populations in states other than the initial one were negligible, whereas the production of either atom pairs in the $|2,\pm 1\rangle$ state or in the $|2,\pm 2\rangle$ state produced by the spin exchange caused by collisions between two $m_F=0$ atoms was favored energetically for the total internal Zeeman energy. In the 3-G magnetic field, the release energies correspond to 31 nK per atom for the production of a $|2,\pm 1\rangle$ atom pair and 124 nK per atom for the production of a $|2,\pm 2\rangle$ atom pair. This result suggests that the spin-mixing dynamics within the $F=2$ manifold is for some reason suppressed under the magnetic field strength conditions.

The number of $|2,0\rangle$ atoms in the trap rapidly decreased [Fig. 1(b)] in comparison with those in the stretched state ($|2,-2\rangle$) due to hyperfine-changing inelastic collisions such as $|2,0\rangle + |2,0\rangle \rightarrow |1,m_F\rangle + |F,m'_F\rangle$ (here $F=1,2$). If the converted atoms had acquired an amount of kinetic energy corresponding to the energy difference between the hyperfine states $F=1$ and 2, they would certainly have escaped from the trap. The loss of atoms from the trap can be described by a differential equation as follows:

$$\frac{dN}{dt} = -(K_1 + K_2\langle n \rangle + K_3\langle n^2 \rangle)N, \quad (3)$$

where N is the number of atoms and K_1 is a rate coefficient for density-independent losses such as residual gas scattering

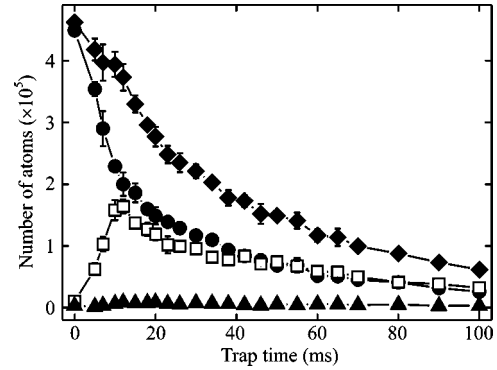


FIG. 2. Number of atoms in the $|2,0\rangle$ (solid circles), $|2,\pm 1\rangle$ (open squares), and $|2,\pm 2\rangle$ (solid triangles) states, as a function of trap time at a magnetic field strength of 1.5 G. The total number of atoms (solid diamonds) is also shown. Each point represents the average of five measurements. Error bars indicate the standard deviation.

and light absorption. K_2 and K_3 represent the decay rates for inelastic two- and three-body collisions, and n is the density of condensates. For K_2 , we obtained a value of $2.1(2) \times 10^{-13} \text{ cm}^3 \text{ s}^{-1}$ by fitting Eq. (3) to the data, where K_1 and K_3 terms were ignored because their contribution to the decay was considered to be extremely small. If a decay curve is drawn using the measured values for $K_1=0.25 \text{ s}^{-1}$, $K_2=2.1 \times 10^{-13} \text{ cm}^3 \text{ s}^{-1}$, and $K_3=1.8 \times 10^{-29} \text{ cm}^6 \text{ s}^{-1}$ [23], we can see that it overlaps with the fitted curve shown in Fig. 1(b) within the resolution of this plot. The value obtained for K_2 is in fair agreement with the upper limit measured to be $3 \times 10^{-13} \text{ cm}^3 \text{ s}^{-1}$ by the JILA group for ^{87}Rb condensates in $|2,1\rangle$ state in a magnetic trap [24].

We also performed the same measurements at magnetic field strengths of 1.5, 1.0, 0.75, 0.5, 0.3, and 0.1 G. Figure 2 shows the number of atoms of each component and the total number of atoms as a function of trap time at a magnetic field strength of 1.5 G. The atom number of $|2,\pm 1\rangle$ components rapidly increased for the first 12 ms, then gradually decreased in the same way as the $|2,0\rangle$ component. The $|2,\pm 2\rangle$ components were rarely observed, and the production of these components through both the first and second terms in Eq. (1) was fully suppressed in this magnetic field.

Although we observed similar evolutions for each component in the 1.0-G magnetic field, a dramatic change in spin mixing occurred after exposure to magnetic fields in the range of 0.75–0.3 G. Figure 3 illustrates the evolution of relative populations for magnetic fields of 1.5, 0.75, 0.3, and 0.1 G. At a magnetic field strength of 0.75 G [Fig. 3(b)], oscillations in the relative populations of $|2,0\rangle$ and $|2,\pm 1\rangle$ components were clearly observed for the first 20 ms. Although similar spinor oscillations have been observed in other studies [13,14], these studies have only reported oscillation time scales over the range from 100 to 200 ms. In the present study, trap time measurements of more than 100 ms could not be investigated because of the limited sensitivity of the charge-coupled-device (CCD) camera. This phenomenon in spin-mixing dynamics has been predicted theoretically for spin-1 condensates in the absence of a magnetic field [7,25].

As shown in Fig. 3(b), the $|2,\pm 2\rangle$ components are produced very slowly, and the kinetic energy obtained by atoms

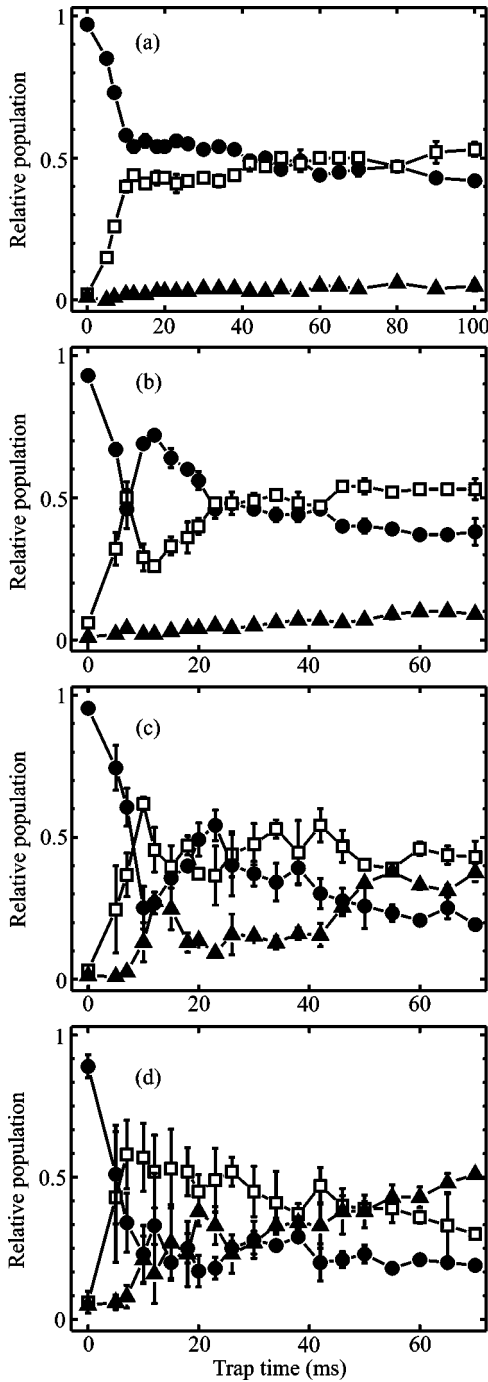


FIG. 3. Relative populations in the $|2,0\rangle$ (solid circles), $|2,\pm 1\rangle$ (open squares), and $|2,\pm 2\rangle$ (solid triangle) states, as a function of trap time at magnetic field strengths of 1.5 G (a), 0.75 G (b), 0.3 G (c), and 0.1 G (d). Each point represents the average of five measurements. Error bars indicate the statistical error.

converted through the $|2,+1\rangle+|2,-1\rangle\rightarrow|2,+2\rangle+|2,-2\rangle$ process is fairly small (6 nK/atom). This characteristic of spin-mixing dynamics demonstrates that the production of $|2,0\rangle$ atom pairs is favored by the $|2,+1\rangle+|2,-1\rangle$ collision process at a magnetic field strength of 0.75 G. This observation is interesting considering that endothermic processes ($|2,+1\rangle+|2,-1\rangle\rightarrow 2\times|2,0\rangle$) are favored (leading to a reduction in the temperature of the whole system); however,

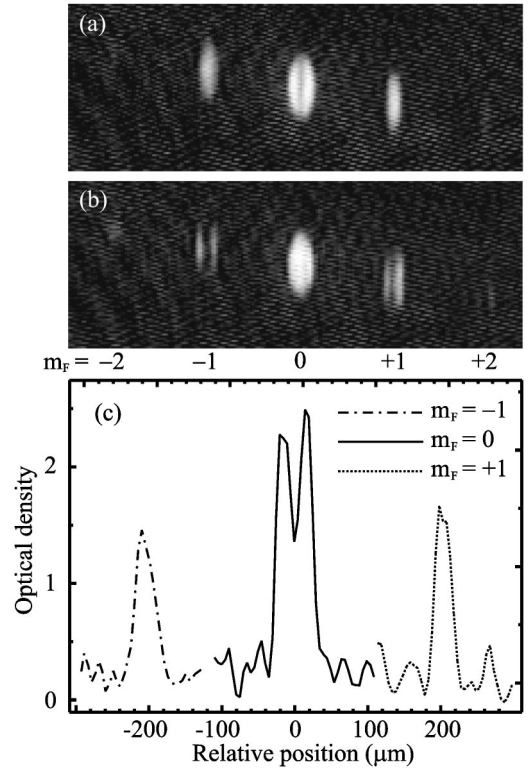


FIG. 4. Images taken after evolutions of 7 ms (a) and 10 ms (b) in a magnetic field strength of 0.75 G. The dips in the density distributions of the condensed atoms are shown in the center of the condensates in the vertical direction for the $|2,0\rangle$ component (a) and the $|2,\pm 1\rangle$ components (b). The size of the field of view for each image is 1.0×0.4 mm. (c) Horizontal profiles of each component in (a) were cut at the center in the vertical direction.

this did not occur at a magnetic field strength of 0.3 G [Fig. 3(c)].

In addition, we observed dips in the density distributions of condensed atoms as shown in Fig. 4. At a trap time of 7 ms, the dip was seen at the center of the condensate in the $|2,0\rangle$ state [Figs. 4(a) and 4(c)] and subsequently appeared in the $|2,\pm 1\rangle$ components at a trap time of 10 ms [Fig. 4(b)]. This indicates that the spin-mixing dynamics developed more frequently in the higher-density regions of the condensates. Similar phase separations have also been observed for the $F=1$ spinor condensates of Na atoms in the equilibrium condition [10]. However, the atom defects shown here are considered to be transitional structures because the system did not reach equilibrium.

At a magnetic field strength of 0.3 G [Fig. 3(c)], the initial decrease in the relative population of the $|2,0\rangle$ component was larger than was observed at 0.75 G. The population of $|2,\pm 1\rangle$ components also increased. In addition, the relative population of $|2,\pm 2\rangle$ components increased, and population oscillations were clearly observed for these components. Furthermore, a delay in the population gain was observed for the $|2,\pm 2\rangle$ components; i.e., the relative population for $|2,\pm 2\rangle$ components began to increase at a trap time of 7 ms. A similar time delay has also been reported by Ref. [13]. This result indicates that increased spin exchange occurs at lower magnetic field strength. In addition, it was

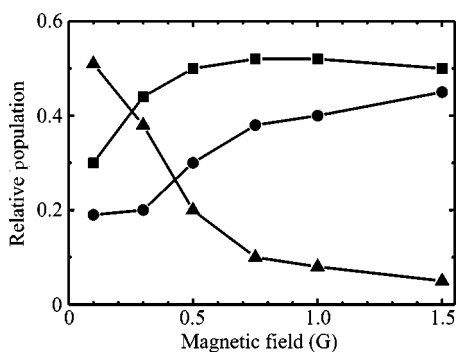


FIG. 5. Relative populations of each spin component after 70 ms storage time in the optical trap represented as a function of the various magnetic field strengths. Solid circles indicate the $|2,0\rangle$ component, solid squares the $|2,\pm 1\rangle$ component, and solid triangles the $|2,\pm 2\rangle$ component.

demonstrated that the spin exchange develops mainly between neighbor states; i.e., $|2,\pm 1\rangle$ components are first converted from the $|2,0\rangle$ component, and then $|2,\pm 2\rangle$ components are produced from the $|2,\pm 1\rangle$ components. This shows that the contribution of the c_2 term in Eq. (1) is extremely small for ^{87}Rb spin-2 condensates.

Comparing Figs. 3(b) and 3(c), the *swinging back* of the $|2,0\rangle$ component population reached a peak at a trap time of about 10 ms in a 0.75-G magnetic field, whereas at 0.3 G, the peak occurred at a trap time of about 20 ms. We suppose that this slowdown in the oscillation is caused by an increase in the population of $|2,\pm 2\rangle$ components. Population oscillations were not observed at a magnetic field strength of 0.1 G [Fig. 3(d)]. However, the tendency in the evolution of relative populations was consistent with the result for the 0.3-G magnetic field strength.

The standard deviations of each of the data points were found to increase at lower magnetic field strengths. Under weak stray ac magnetic fields, the off-resonant rf transitions between different Zeeman states can take place [14]. Thus, it is possible that these ac magnetic fields affect the relative population distribution between different m_F components. This effect might also increase with a decrease in the strength of the external dc magnetic field. We searched for these fields using a Hall probe magnetometer and by measuring the evolution of optically trapped condensates in the $|2,-2\rangle$ state. However, we did not detect any ac magnetic fields. We suppose that the increase in the fluctuation of populations might have resulted from small population oscillations occurring on a faster time scale than the time interval employed for our measurements.

Ground-state structure and magnetization of ^{87}Rb spin-2 condensates were deduced from the magnetic field dependence of their spinor dynamics. Figure 5 illustrates the relative populations for each component measured after a trap time of 70 ms, as a function of the magnetic field strength. The relative population of $|2,\pm 2\rangle$ components increases with a decrease of magnetic field strength, while populations of the other components decreased. One of the ground states of spin-2 condensates with antiferromagnetic properties in the absence of a magnetic field is predicted to be a mixture of $|2,-2\rangle+|2,+2\rangle$ [18]. However, if a cyclic phase is the

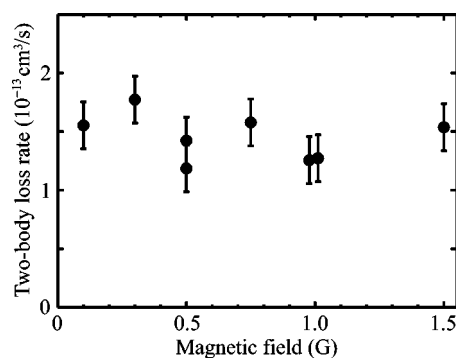


FIG. 6. Loss rates for an inelastic two-body collision at various magnetic field strengths. The values were determined by fitting Eq. (3) and omitting the K_1 and K_3 terms for the evolution of the total number of atoms in each data set. At a magnetic field strength of 1.0 G, the data points were plotted separately because the two values were very close. The magnitude of the error for each point was dependent on the error in the measured trap frequency, which was estimated to be 8 Hz.

ground state of the system, the configuration of $|2,-2\rangle+|2,0\rangle+|2,+2\rangle$ is stable [13]. Our system did not completely reach equilibrium conditions within the time scale investigated. Nevertheless, the tendency of the magnetic field dependence of the spinor dynamics demonstrates an antiferromagnetic nature for the ^{87}Rb spin-2 condensates investigated in this study.

Finally, we illustrated the loss rates due to the inelastic two-body collisions measured for the various magnetic fields (Fig. 6). The values were obtained by fitting Eq. (3) and omitting the terms K_1 and K_2 for the evolution of the total number of atoms. No obvious dependence of the loss rates on the magnetic field strength observed. This indicates that spin-mixing dynamics does not contribute to the trap loss and evolve in the hyperfine spin state of the $F=2$ manifold. The mean value of $1.4(2) \times 10^{-13} \text{ cm}^3 \text{ s}^{-1}$ is in fair agreement with the value reported by [13].

V. CONCLUSIONS

We studied the dynamics of optically trapped ^{87}Rb spin-2 condensates. Although the condensed atoms in the non-stretched state and the mixture of different m_F components were lost from the trap at high rates due to hyperfine-changing collisions, spin-mixing processes between different m_F components were observed at various magnetic field strengths. The population oscillation of the m_F components during the evolution of spin mixing was also observed. In addition, we found that this phenomenon occurred only at specific magnetic field strengths. We also demonstrated that the spin-dependent interactions occurred in the high-density regions of the spinor condensates. By observing the tendency for relative populations of each of the m_F components after 70 ms time evolution in the optical trap at various magnetic field strengths, we deduced that the ^{87}Rb spin-2 condensate had antiferromagnetic properties. We also confirmed that no external trap losses occurred during the spin-mixing process

for magnetic field strengths from 0.1 to 1.5 G. Our future work will involve studies of the spinor dynamics of this system at near-zero magnetic field strength, using an improved apparatus. Such studies are likely to improve our knowledge of the magnetic properties of this system. We also plan to study the mixture of $F=1$ and $F=2$ spinor condensates to probe the interactions between the spinor condensates affected by different magnetization.

ACKNOWLEDGMENTS

We would like to thank M. Ueda for many valuable discussions and Y. Torii, Y. Yoshikawa, K. Itoh, Y. Sasaki, K. Kondo, and N. Kikuchi for assistance during the early stages of the experiment. This work was supported by a Grant-in-Aid from the Scientific Research by the Ministry of Education, Science, Sport, and Culture of Japan. Additional funding was provided by CREST, JST.

-
- [1] C. J. Myatt, E. A. Burt, R. W. Ghrist, E. A. Cornell, and C. E. Wieman, *Phys. Rev. Lett.* **78**, 586 (1997).
 - [2] M. R. Matthews, D. S. Hall, D. S. Jin, J. R. Ensher, C. E. Wieman, E. A. Cornell, F. Dalfovo, C. Minniti, and S. Stringari, *Phys. Rev. Lett.* **81**, 243 (1998).
 - [3] M. R. Matthews, B. P. Anderson, P. C. Haljan, D. S. Hall, C. E. Wieman, and E. A. Cornell, *Phys. Rev. Lett.* **83**, 2498 (1999).
 - [4] J. M. McGuirk, H. J. Lewandowski, D. M. Harber, T. Nikuni, J. E. Williams, and E. A. Cornell, *Phys. Rev. Lett.* **89**, 090402 (2002).
 - [5] T. Ohmi and K. Machida, *J. Phys. Soc. Jpn.* **67**, 1822 (1998).
 - [6] T.-L. Ho, *Phys. Rev. Lett.* **81**, 742 (1998).
 - [7] C. K. Law, H. Pu, and N. P. Bigelow, *Phys. Rev. Lett.* **81**, 5257 (1998).
 - [8] M. Koashi and M. Ueda, *Phys. Rev. Lett.* **84**, 1066 (2000).
 - [9] D. M. Stamper-Kurn, M. R. Andrews, A. P. Chikkatur, S. Inouye, H.-J. Miesner, J. Stenger, and W. Ketterle, *Phys. Rev. Lett.* **80**, 2027 (1998).
 - [10] J. Stenger, S. Inouye, D. M. Stamper-Kurn, H.-J. Miesner, A. P. Chikkatur, and W. Ketterle, *Nature (London)* **396**, 345 (1998).
 - [11] H.-J. Miesner, D. M. Stamper-Kurn, J. Stenger, S. Inouye, A. P. Chikkatur, and W. Ketterle, *Phys. Rev. Lett.* **82**, 2228 (1999).
 - [12] D. M. Stamper-Kurn, H.-J. Miesner, A. P. Chikkatur, S. Inouye, J. Stenger, and W. Ketterle, *Phys. Rev. Lett.* **83**, 661 (1999).
 - [13] H. Schmaljohann, M. Erhard, J. Kronjäger, M. Kottke, S. van Staa, J. J. Arlt, K. Bongs, and K. Sengstock, *Phys. Rev. Lett.* **92**, 040402 (2003).
 - [14] M.-S. Chang, C. D. Hamley, M. D. Barrett, J. A. Sauer, K. M. Fortier, W. Zhang, L. You, and M. S. Chapman, *Phys. Rev. Lett.* **92**, 140403 (2004).
 - [15] C. V. Ciobanu, S.-K. Yip, and T.-L. Ho, *Phys. Rev. A* **61**, 033607 (2000).
 - [16] T.-L. Ho and L. Yin, *Phys. Rev. Lett.* **84**, 2302 (2000).
 - [17] N. N. Klausen, J. L. Bohn, and C. H. Greene, *Phys. Rev. A* **64**, 053602 (2001).
 - [18] M. Ueda and M. Koashi, *Phys. Rev. A* **65**, 063602 (2002).
 - [19] A. Görlitz, T. L. Gustavson, A. E. Leanhardt, R. Löw, A. P. Chikkatur, S. Gupta, S. Inouye, D. E. Pritchard, and W. Ketterle, *Phys. Rev. Lett.* **90**, 090401 (2003).
 - [20] J. L. Roberts, J. P. Burke, N. R. Claussen, S. L. Cornish, E. A. Donley, and C. E. Wieman, *Phys. Rev. A* **64**, 024702 (2001).
 - [21] Y. Takasu, K. Honda, K. Komori, T. Kuwamoto, M. Kumakura, Y. Takahashi, and T. Yabuzaki, *Phys. Rev. Lett.* **90**, 023003 (2003).
 - [22] M.-O. Mewes, M. R. Andrews, D. M. Kurn, D. S. Durfee, C. G. Townsend, and W. Ketterle, *Phys. Rev. Lett.* **78**, 582 (1997).
 - [23] J. Söding, D. Guéry-Odelin, P. Desbiolles, F. Chevy, H. Inamori, and J. Dalibard, *Appl. Phys. B: Lasers Opt.* **69**, 257 (1999).
 - [24] M. R. Matthews, Ph.D. thesis, University of Colorado, 1999.
 - [25] H. Pu, C. K. Law, S. Raghavan, J. H. Eberly, and N. P. Bigelow, *Phys. Rev. A* **60**, 1463 (1999).